



# Flow and tracer transport in a single fracture at non-isothermal conditions

Yashar Tavakkoli Osgouei<sup>1,2</sup> · Serhat Akin<sup>1</sup>

Received: 15 October 2021 / Accepted: 19 November 2022 / Published online: 25 November 2022  
© Saudi Society for Geosciences 2022

## Abstract

Assessing preferential flow that occurs through small fractures or permeable connected pathways of other kinds is important to many processes but is difficult to determine, since most chemical tracers diffuse quickly enough from small flow channels that they appear to move more uniformly through the rock than they actually do. Conventional tracer and micro tracer experiments were conducted using two different synthetically single-fractured limestone core plugs to investigate non-isothermal-coupled heat and mass transfer in a single fracture-matrix system. Conventional Rhodamine B and suspension of micro particles based on melamine resin, Rhodamine B-marked size 1- $\mu\text{m}$  tracer with constant concentration were injected at constant flow rate during non-isothermal flow-through experiments. Effluent tracer concentrations were measured using the fluorescence spectrometry technique. A numerical simulation model was used to determine effective thermal and physical properties involved in matrix-fracture transfers during conventional tracer injection. Numerical studies indicated that matrix permeability is the main controlling factor for tracer dispersion within the matrix. The results showed that tracer transfer from the fracture to the matrix at low injection rates is higher compared to that of higher injection rates. As the fracture provides a large transport pathway for micro particles compared to the surrounding matrix, advection causes the early breakthrough for micro particle transport through a single fracture-matrix system. When the conventional tracer has a long enough transit through the system to diffuse into the matrix, but the micro tracer does not, the micro tracer arrives first and the conventional tracer later, and the separation measures the degree of preferential flow.

**Keywords** Fractured porous media · Matrix-fracture transfers · Micro tracers · Tracer testing modeling · Non-isothermal solute transport · Geothermal reservoir engineering

## Introduction

Matrix-fracture transfers received considerable interest in recent years because of numerous applications in different fields of study such as agricultural, chemical, hydrological, environmental, petroleum, and geothermal engineering (Olasolo et al. 2016). The intricate structure of matrix-fracture systems in the sense of the spatial distribution of physical heterogeneities necessitates the use of different models of

flow and transport along fractured porous media (Berre et al. 2019; Kumar 2012). Fractured porous media comprise the high-permeability domain in fracture with advection transport mechanism as opposed to the low-permeability domain of matrix with dispersion and/or molecular diffusion transport mechanism, representing heterogeneous systems (Boon et al. 2017; Sahimi 2011). The heterogeneities in fractured porous media produce complicated fluid velocity profiles. The large velocity difference between fracture and matrix where flow velocity in the fracture is faster than that of the matrix has a profound impact on the nature of flow and transport in fractured porous media (Kumar 2012; Bijeljic et al. 2011). While fluid mainly flows through the fracture, the porous matrix can be a controlling factor in matrix-fracture transfers (Schmelling and Ross 1989). The physical properties of the matrix such as porosity and permeability can contribute to solute transport within the matrix through dispersion in matrix-fracture systems (Boving and Grathwohl

---

Responsible Editor: Santanu Banerjee

✉ Yashar Tavakkoli Osgouei  
yashar.osgouei@gmail.com

<sup>1</sup> Department of Petroleum and Natural Gas Engineering, Middle East Technical University, Ankara, Turkey

<sup>2</sup> Department of Petroleum and Natural Gas Engineering, Near East University, Nicosia, Mersin 10, Turkey

2001). There are many numerical and experimental tracer tests that were carried out to investigate the effects of different properties of matrix and fracture on solute transport in fractured porous media (Grisa and Pickens 1980; Grisak et al. 1980). It was observed that matrix diffusion is effective in altering solute breakthrough curves and concentration profiles in fracture and matrix. Although solute transport in fractured porous media can be considered non-Fickian due to early breakthrough by heterogeneity, the difference of two distinct flow domains leads to considerable solute concentration gradients between fracture and matrix. The solute concentration gradient between matrix and fracture can be a reason for matrix-fracture mass transfer (Geiger et al. 2010; Tsang et al. 1988). In addition to the velocity difference between fracture and matrix, other chemical and physical processes such as dispersion and adsorption within the matrix and over the matrix-fracture interface can inhibit mass transport in fractured porous media (Werth et al. 2006; Khuzhayorov and Mustofokulov 2019; Khuzhayorov and Mustofokulov 2018). The effect of matrix heterogeneity and non-equilibrium adsorption on solute transport and concentration distribution in fractured porous media was investigated numerically. The results indicated that the distribution of solute concentration and adsorption are asymmetric due to matrix heterogeneity (Khuzhayorov et al. 2020).

Over the recent decades, the need for the understanding, characterizing, and modeling of flow and transport as well as interactions within porous media has been increased (Berre et al. 2019). Several different analytical models with differing degrees of complexity have been developed (Grisak and Pickens 1981; Zhu et al. 2016). The results of these models showed that first-order reactions in fracture and matrix and matrix diffusion cause retardation in solute transport. The effect of asymmetric matrix properties on solute transport in the single fracture-matrix system with asymmetric matrix blocks was also studied. It has been concluded that the asymmetric matrix retardation factor was the main reason for the different spatiotemporal distributions of solute in the single fracture-matrix system (Zhu and Zhan 2018). More recently, an experimental and numerical study was conducted to analyze cold water injection through single-fractured core plugs. The results revealed that matrix-fracture heat transfer is dependent not only on flowing conditions in fracture, but also thermal properties of the matrix at non-isothermal conditions. In fact, thermal properties of the matrix play a crucial role in the establishment of temperature over the fracture surface, in turn, assigning the temperature gradient between fracture fluid and fracture surface (Tavakkoli Osgouei and Akin 2021).

A large number of studies were devoted to investigating the effects of the physical properties of the matrix and flow characteristics in fracture on solute transport through matrix-fracture systems. In these studies, solute transport

was carried out through single fracture-matrix systems at isothermal conditions. However, simultaneous heat and mass transfer over solute transport through matrix-fracture systems at non-isothermal conditions have not received great attention because of complexities, which result in large-scale variations in flow and transport properties. Investigation of matrix-fracture mass transfer has been accomplished using several non-isothermal tracer injection experiments conducted using single-fractured limestone core plugs. A numerical simulation model calibrated with effluent tracer concentration was used to determine anisotropic values of dispersion coefficient for different single fracture-matrix systems. As opposed to the aforementioned studies where tracer concentrations of fracture and fracture surface were assumed to be equal, the developed numerical simulation model considers the concentration difference between fracture and fracture surface for non-isothermal tracer injection. Heat transfer during cold water injection was considered by assigning variable matrix properties such as thermal conductivity and volumetric heat capacity (Tavakkoli Osgouei and Akin 2021). In addition to the effect of the physical properties of the matrix on mass transfer by dispersion or diffusion within the matrix, thermal matrix properties can contribute mass transfer in the matrix-fracture system due to temperature gradient between fracture surface and the fluid. Thus, coupled heat and mass transfer were used to describe matrix-fracture transfer for non-isothermal conditions including the Soret effect.

## Soret effect

The analysis of coupled heat and mass transfers through porous media is required for modeling flow in fractured petroleum and geothermal reservoirs. Matrix-fracture transfer in non-isothermal conditions can be evaluated by coupling heat and mass transfers (Reddy and Govardhan 2015). Transient and steady heat flows can be coupled with solute transport, either implicitly as natural convection incorporating the effect of thermal flux on the variation of concentration gradients, or explicitly as a “Soret effect,” where the divergence of the thermal flux acts as an additional source term affecting the change of solute concentration (Reddy and Rao 2012; Reddy et al. 2010). In brief, the thermal properties of the matrix along with the physical properties of the matrix where dispersion/diffusion processes within the matrix lead to changes in the outlet concentration and concentration profile along fracture should be considered when modeling non-isothermal tracer injection processes in matrix-fracture systems. The effect of the thermal properties of the matrix on mass transfer by the Soret effect cannot be underestimated. In fact, the Soret effect, which occurs in form of solute migration in matrix-fracture systems as

a result of the temperature gradient between fracture fluid and fracture surface, can contribute to matrix–fracture mass transfer over a matrix–fracture interface. It changes the concentration profile of solute along fracture over the duration of the tracer injection experiments in non-isothermal conditions. Figure 1a indicates the schematic representation of the Soret effect due to the temperature gradient between the fracture surface and fluid in fracture over tracer injection at non-isothermal conditions through the single-fractured core plug.

## Material and methods

### The single fracture–matrix system

The two single-fractured limestone core plugs prepared artificially were used to investigate simultaneous heat and mass transfers in non-isothermal conditions. A synthetic single fracture–matrix system was created by cutting each of these cylindrical core plugs along their lengths. The physical properties of the core plugs used in the present study are given in Table 1. To measure heat transfer and the temperature in the fracture during tracer injection, a thin film–type heat flux sensor (Omega HFS 3 with a sensitivity of  $\pm 10\%$ ) is placed at the fracture in the middle of each core plug, which was then sealed with epoxy resin to create a no-flow boundary condition at the radial boundary (Fig. 1b). As a result, top and bottom of cylindrical halves were separated by a

**Table 1** Physical properties of the limestone core plugs

Core plug	Length (cm)	Diameter (cm)	Porosity (%)	Permeability (md)	Pore volume (cm <sup>3</sup> )
#1	7.21	3.72	17.92	8.39	14.04
#2	7.13	3.72	19.0	3.79	14.73

horizontal fracture with an aperture of 0.01778 cm. Then the fractured core is positioned in a Teflon core holder with two end caps with spider web–shaped grooves at the top and bottom of the core plug allowing fluid to flow in and out of the core holder along its length.

### Experimental setup and procedure

The experimental setup consisted of the aforementioned fractured core holder, a water bath to maintain the temperature of the core plug’s outer surface at the desired temperature (i.e., either at 70 °C or 90 °C), thermocouples (sensitivity  $\pm 2.2$  °C) to measure inlet fluid and water bath temperatures, production collection system, a data logger (Elimko E-680) to record water bath, inlet and fracture temperatures and heat flux, a constant displacement pump (ISCO), and injection–production lines. The schematic of the experimental apparatus is shown in Fig. 2. In all experiments, colder water was injected into the fractured core assembly at one end at constant temperature ( $T_{in}$ ) and constant flow rate (1 ml/min) by a constant displacement pump (ISCO) and accumulated from the other end using a production collection system. The position of the fracture plane and direction of flow was kept horizontal in all experiments. In all experiments, the temperature of the core plug’s outer surface ( $T_o$ ) was maintained at a constant temperature either at 70 °C or 90 °C by using a constant temperature circulating water bath. When the desired initial temperature of the core plug is reached as indicated by the heat flux sensor within fracture ( $T_f$ ), this temperature is kept constant for at least an hour to guarantee that the whole core sample is at constant and uniform temperature condition. After that, colder Rhodamine B solution (conventional tracer) or micro particles based on melamine resin, Rhodamine B–marked size of 1  $\mu$ m suspension (micro tracer) at 30 °C is injected at differing flow rates and injection temperatures using an inlet cap that is connected to a constant displacement pump (ISCO) through the injection line for 5 h. The injection line contains a thermocouple to measure the water temperature ( $T_{in}$ ) at the inlet line of the fractured core assembly. The other end of the fractured core assembly is connected to a production collection system through a production line. Fracture temperature and the heat flux to and out of the fracture are measured by a film–type heat flux sensor (Omega HFS 3 with a sensitivity

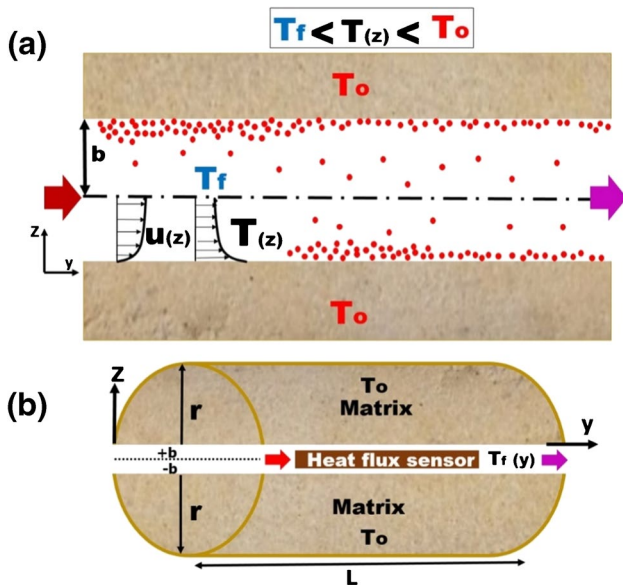


**Fig. 1** a The Soret effect and temperature gradient in non-isothermal tracer injection, the red dots represent solute tracer migration from fracture fluid to fracture surface. b A sketch of a single-fractured core plug used in the fracture–matrix transfer study.

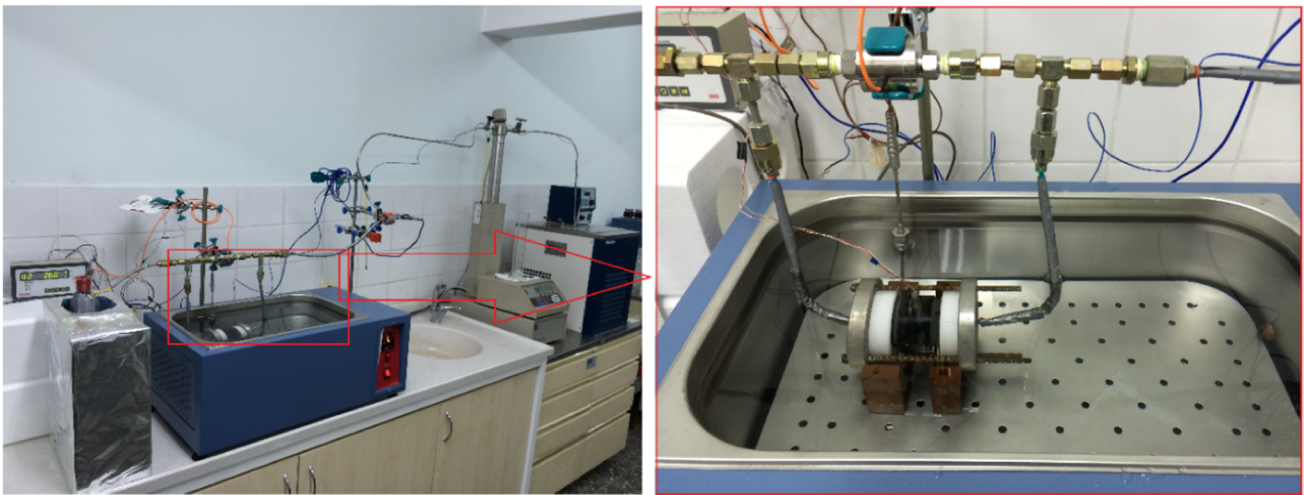
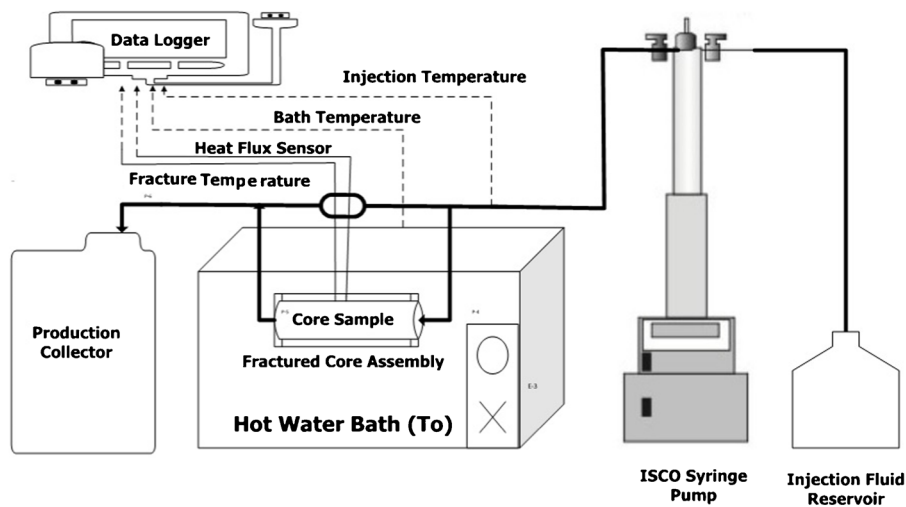


**Fig. 2** Schematic drawing (top) and photos (bottom) of the experimental setup used in tracer injection experiments

of  $\pm 10\%$ ). Core inlet, outlet, and heating-circulator bath temperatures were measured using J-type thermocouples using an interval of 5 min. Water leaves the fractured core, accumulating in the production collection system. The measurement frequency of the fracture temperature and water inlet temperature in addition to heat flux between matrix and fracture is kept constant at 5 min by means of a digital data logger. The tracer concentration of each collected sample is then measured using a fluorometer (Turner Quantech Digital Filter Fluorometer Model NO. FM109510-33).

### Mathematical description of matrix-fracture solute transport

In fractured porous media, fluid mainly flows through fracture due to marked differences in physical pore-scale properties such as permeability and specific storage between matrix and fracture. Even though high permeability fracture

provides the major flow path for solute transport, the rock matrix adjacent to the fracture is an important part of the overall solute transport process (Bodin et al. 2003). The solute transport mechanism along the fracture is advection while dispersion or diffusion is predominant within the matrix. In addition, solute diffusion is possible along the matrix-fracture interface as well. For simplicity, it is assumed that diffusion within the matrix over the length of the core plug and longitudinal dispersion in the fracture is negligible. The physical properties of rock matrix such as porosity and permeability may affect solute transport in the matrix-fracture system through the dispersion coefficient (Boving and Grathwohl 2001). The fracture dispersion coefficient can be defined as follows (Zou et al 2016).

$$D = D_f = a_L u_y + D_m \quad (1)$$

where  $D_f$  is the dispersion coefficient in fracture;  $a_L$  is the longitudinal dispersivity along the fracture;  $u_y$  is the fluid velocity in fracture;  $D_m$  is the molecular diffusion coefficient of solute in the fracture fluid. For the porous matrix ( $u=0$ ): the dispersion coefficient is considered the effective diffusion coefficient ( $D_e$ ).

$$D = D_e = \tau D_m \tag{2}$$

where  $D_e$  is the effective diffusion coefficient of the matrix;  $\tau$  is the tortuosity of the matrix;  $D_m$  is the molecular diffusion coefficient of the solute. The solute transport in the fracture can be defined with the following equation (Zhu et al. 2016; Zou et al 2016).

$$\frac{\partial C_f}{\partial t} + u \frac{\partial C_f}{\partial y} - D_f \frac{\partial^2 C_f}{\partial y^2} - \frac{\phi D_e}{b} \frac{\partial C_m}{\partial Z} \Big|_{z=\pm b} = 0 \tag{3}$$

where  $C_f$  is the solute concentration in the fracture;  $u$  is the fluid velocity in fracture;  $D_f$  is the dispersion coefficient in the fracture;  $D_e$  is the effective diffusion coefficient of the matrix;  $b$  is the fracture half aperture;  $C_m$  is the solute concentration in the rock matrix. For non-reactive solute transport with a constant concentration source and negligible longitudinal dispersion in the fracture, Eq. (3) can be simplified as follows.

$$\frac{\partial C_f}{\partial t} + u \frac{\partial C_f}{\partial y} - \frac{\phi D_e}{b} \frac{\partial C_m}{\partial Z} \Big|_{z=\pm b} = 0 \tag{4}$$

Moreover, if transverse diffusion within the matrix is dominant, solute transport can be further simplified.

$$\frac{\partial C_m}{\partial t} = D_e \frac{\partial^2 C_m}{\partial Z^2} \tag{5}$$

Assuming that solute concentrations in the fracture and at the fracture surface are equal along the matrix-fracture interface, the following initial and boundary conditions can be defined (Grisak and Pickens 1981; Zhu et al. 2016).

$$C_f(y = 0, t) = C_o \tag{6}$$

$$C_f(y, t = 0) = 0 \tag{7}$$

The solution of solute transport equations can be obtained as:

$$\frac{C_f(y, t)}{C_o} = \operatorname{erfc} \left[ \frac{\frac{\phi D_e}{ub} y}{2\sqrt{\frac{D_e}{u}(ut - y)}} \right] \text{ if } t > y/u \tag{8}$$

**Table 2** Type and dimension of the grid system in the numerical simulation model

Rock type	Color	Position		
		X	Y	Z
Matrix	Blue	1:15	1:120	2:26
Fracture	Red	1:15	1:37	1
			84:120	
Sensor	Yellow	1:15	38:83	1

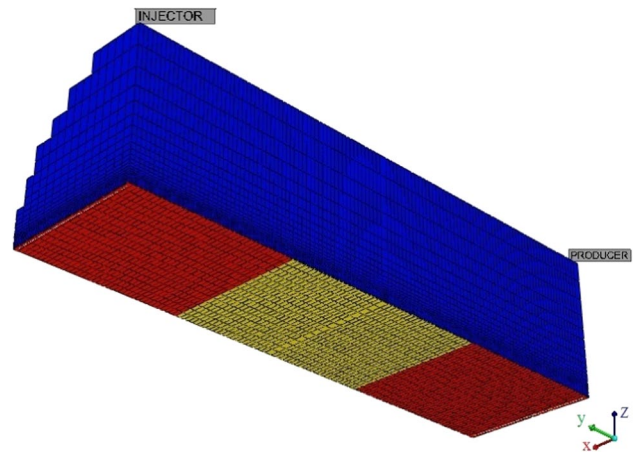


**Fig. 3** A quarter of the 3D numerical simulation model of the single fracture-matrix system

### Numerical simulation model

To investigate coupled heat and mass transfer along the matrix-fracture interface due to cold solute injection, a numerical simulation model of the single fracture-matrix system was developed. The CMG STARS is a fully implicit, multiphase, and multi component finite difference numerical simulator that can be used for modeling thermal and solute transports in the single matrix-fracture system (CMG STARS Manual 2020). The number of grids is selected to minimize numerical smearing errors. Starting with a small number of grids, several trial and error runs were conducted until numerical smearing errors were minimized. Thus, the gridding system of  $15 \times 120 \times 26$  blocks in  $x$ ,  $y$ , and  $z$  directions respectively provides a proper simulation model to study matrix-fracture transfers (Table 2 and Fig. 3). Assuming symmetry, a quarter of the fractured core plug with a total of 46,800 grid numbers in various sizes was used. To the best of our knowledge, the current gridding scheme also ensures the stability of the solution. No attempt has been carried out to use alternative gridding schemes such as Voronoi grids or further increase in the number of grids. The model was populated by assigning different values of porosity and permeability for matrix, fracture, and sensor

sections. Matrix permeability and porosity were experimentally measured before cutting the core plug and installing a heat flux sensor. The analytical model derived from the solution of solute transport equations was used to populate the initial distribution of solute concentration in isothermal conditions. Fracture permeability and porosity along with matrix thermal properties (matrix volumetric heat capacity and thermal conductivity) and matrix dispersion coefficients in different directions (anisotropic dispersion coefficients  $D_x$ ,  $D_y$ ,  $D_z$ ) were determined by calibrating the numerical simulation model with measured values of fracture temperature and outlet concentration. Matrix porosity, matrix permeability, capillary pressure, and initial temperatures were assumed to be constant. Matrix volumetric heat capacity, thermal conductivity, and matrix dispersion coefficients were iteratively modified until a satisfactory match of the numerical model output with the experimental measurements was achieved. The calibration determines a valid set of model parameters that enable the use of a simulated model for the prediction of flow and/or transport behavior for different scenarios of matrix-fracture transfers in non-isothermal conditions (Tunish et al. 2019).

## Results and discussion

### Experimental measurements of conventional tracer solutions

The effluent samples were collected at regular time intervals (i.e. 5 min) to measure Rhodamine B concentrations by a digital fluorometer. Figure 4 shows tracer breakthrough curves for core plugs #1 and #2 at an initial temperature of 70 °C for a flow rate of 1 (ml/min). As the tracer is gradually introduced in the fracture, a portion of the tracer propagates into the porous matrix by dispersion over the duration of the tracer injection experiment. As time goes on, the effluent concentration increases in both experiments. This increase shows that advection is a predominant mechanism of solute transport in a single-fractured core plug while a small portion of the influent tracer penetrates into the matrix as a result of dispersion. As time progresses, the matrix storage capacity (pore volume) is gradually utilized causing more matrix saturated by tracer solution. The outlet concentration continues to increase until equilibrium is established between the solute moved to the matrix and the solute flowing in the fracture. Finally, the effluent tracer concentration hovers around a relatively steady value for the rest of the tracer injection experiment. As revealed by the experimental tracer breakthrough curves, steady values of outlet concentration depend on the physical properties of the porous matrix,

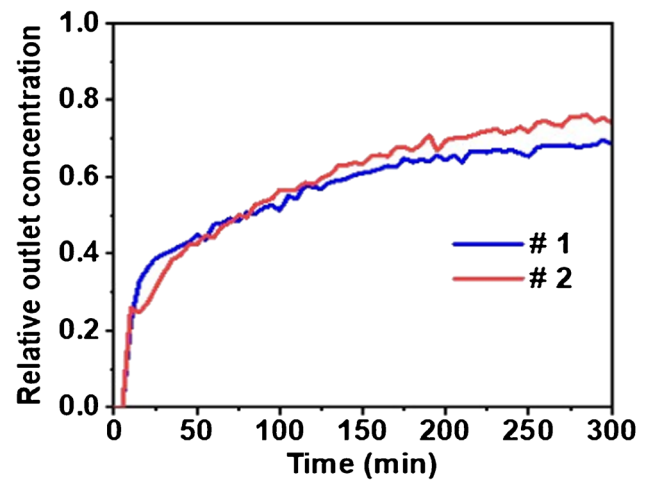


**Fig. 4** Experimental conventional tracer breakthrough curves for a flow rate of 1 ml/min at an initial temperature of 70 °C for different core plugs (Relative outlet concentration = outlet concentration of tracer/tracer concentration injected)

especially, matrix permeability. If the matrix permeability is relatively large but somewhat smaller than the fracture permeability, low effluent concentrations are expected. In this regard, core plug #2 with lower matrix permeability has a larger relative effluent concentration compared to that of core plug #1. Large effluent concentration shows that less solute penetrates into the matrix through the dispersion mechanism. Consequently, dispersion is a determinant factor in predicting the value of final concentration in a single fracture-matrix system. The difference in effluent tracer concentrations can be considered an indicator of mass transfer in the matrix-fracture interface (Fig. 5a). The main reason for oscillatory trends is the presence of reversible and reciprocal movement of solute between porous matrix and fracture. As can clearly be seen that the amplitude of these oscillations is high during the early time, decreasing eventually as equilibrium is reached. In other words, the solute moves from fracture to matrix and then from matrix to fracture, respectively.

Experimental values of heat flux over matrix-fracture interface were measured to analyze single fracture-matrix solute transfer. Figure 5b represents the oscillatory trends for heat flux between matrix and fracture similar to those observed for tracer concentration. These oscillations in heat flux can come from the reversible motion of colder fluid injected due to temperature gradient along the matrix-fracture interface. In fact, some colder fluid penetrates the hot matrix and then moves back to fracture trying to reach thermal equilibrium. This triggers mass transfer between fracture and matrix as seen in Fig. 5a.

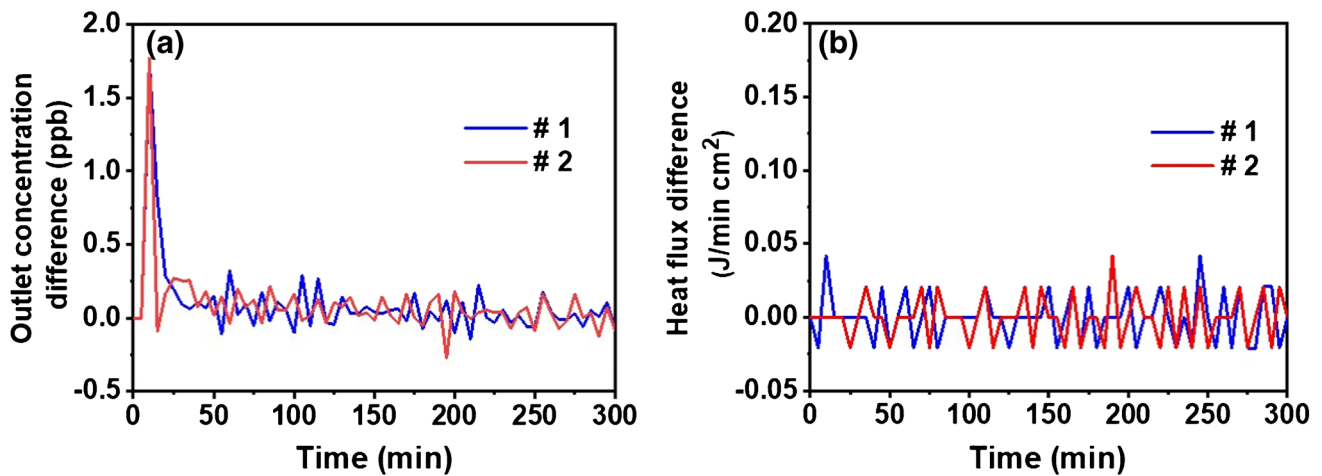


**Fig. 5** **a** Outlet concentration and **b** heat flux changes for a flow rate of 1 ml/min at an initial temperature of 70 °C for different core plugs (Outlet concentration difference refers to forward time finite difference of outlet concentrations).

### Experimental measurements of micro tracer solutions

In order to investigate transport in matrix-fracture system, Rhodamine B micro particles with an average size of 1  $\mu\text{m}$  (mark of Sigma-Aldrich) based on melamine resin that is made up of an aqueous polycondensation of methylol melamine without surfactants were used. The density of micro particles is 1.5 (g/cm<sup>3</sup>) with thermal stability up to 300 °C. As micro particles of Rhodamine B in tracer suspension have induced fluorescence, the concentration measurements of micro particle suspensions were carried out by the fluorescence spectrometry similar to conventional Rhodamine B solutions. Thus, Turner Quantech Digital Filter Fluorometer Model NO: FM109510-33 was used to measure the concentration of samples collected during experiments. The effluent micro particle Rhodamine B samples were collected at regular time intervals (i.e., 5 min).

Figure 6 shows micro particle tracer breakthrough curves for different core plugs at a temperature of 70 °C and an injection rate 1 (ml/min) for 5 h (300 min). The breakthrough times of micro particles suspensions are faster than that of conventional Rhodamine B in all fractured core plugs. The shape of micro particle breakthrough curve gives detailed information about matrix-fracture transfers and mechanisms involved in particle transport through fractured porous media. As the fracture provides large transport pathway for micro particles compared to the surrounding matrix, advection as the predominant mechanism causes the early breakthrough for micro particle transport through a single fracture-matrix system. In fact, the lack of micro particle penetration into the surrounding matrix due to lower permeability of the matrix, smaller pore throat size of matrix relative to particle size, and similar charge of particles can

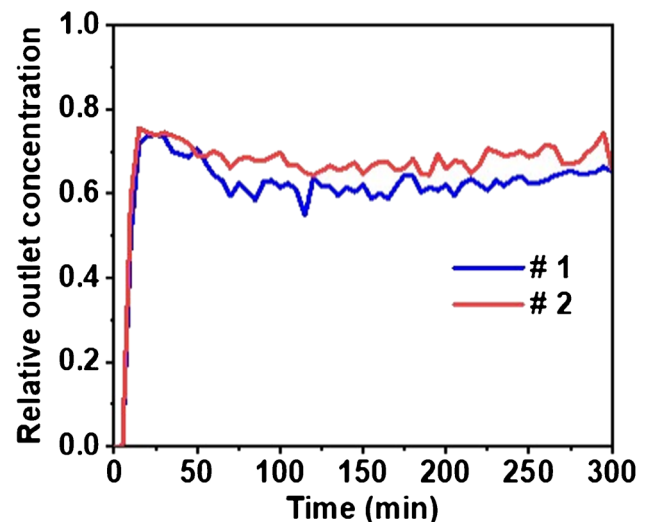


**Fig. 6** Experimental micro particle tracer breakthrough curves for a flow rate of 1 ml/min at an initial temperature of 70 °C for different core plugs

be considered the main reasons for decreasing collision with the matrix grains and fast-moving streamlines in fracture and thus faster breakthrough for micro particles. No spread in the breakthrough curve because of lower attachment of micro particles to matrix grains results in the plug flow form in breakthrough curve. The reason behind this observation is the size exclusion effect, whereby larger tracer particles are excluded from small pores and are therefore transported with higher average velocity, which is pore size-dependent. Since the micro tracer particles cannot diffuse into the matrix, the micro tracer particle breakthrough faster compared to the conventional tracer. In this regard, the average velocity estimated with rhodamine is lower than the velocity of the

fluorescent particles. The separation between breakthrough times measures the degree of preferential flow.

Similar to tracer testing by Rhodamine B solution injection, the values of heat flux in matrix-fracture interface and temperature in the middle of fracture were measured by a heat flux sensor during the micro particle suspension injection at a flow rate 1 (ml/min) and outer temperature 70 °C (Fig. 7a and b). In view of the somewhat lower injection rate of 1 (ml/min) of micro particle suspension, the values of heat flux and temperature in fracture hover around the same level in all experiments suggesting a similar mechanism to those observed for conventional tracer injection.

### Calibration of matrix-fracture transfer model

The history matching of experimental data was carried out using CMG-STARs simulator. To calibrate the numerical model of solute transport, data from conventional tracer injection experiments were assumed as validation data. The analytical model diffusion coefficient ( $D_e$ ) is used as the initial guess of the numerical model parameters. In order to obtain the analytical diffusion coefficient, the aforementioned analytical model and experimental concentrations are matched by minimizing the sum of the square of differences using Microsoft Excel's non-linear solver (Ramírez-Sabag et al. 2005). The fitting parameter used to fit the tracer concentration model to experimental measurement is the effective diffusion coefficient ( $D_e$ ) in fractured porous media where the main portion of the fluid is transported through fracture assuming velocity within the porous matrix is close to zero. That is why the matrix dispersion coefficient is considered the effective diffusion coefficient. It increases with increasing matrix permeability (Charette et al. 2007). Core plug #2 has a lower effective diffusion coefficient of 0.59

( $\text{cm}^2/\text{min}$ ) due to less matrix permeability. However, the relatively large matrix permeability of core plug #1 causes a larger effective diffusion coefficient of 0.73 ( $\text{cm}^2/\text{min}$ ) (Table 4).

The experimental measurements of Rhodamine B concentrations in the fracture outlet were used as the basis for numerical simulation. The fracture porosity, fracture permeability, matrix volumetric heat capacity, and matrix thermal conductivity parameters, which are determined by the history matching of the thermal transport model, were considered constant. The values of dispersion coefficient in different directions (anisotropic dispersion coefficients  $D_x$ ,  $D_y$ ,  $D_z$ ) were iteratively modified until a satisfactory match of the numerical simulation output with the experimental measurements was achieved (Table 4). Figure 8a and b compare the results of numerical models calibrated with experimental effluent tracer concentrations measured in a flow rate of 1 (ml/min) at an outer temperature of 70 °C for core plugs #1 and #2. It can be clearly observed that the outlet concentration predicted by the analytical model cannot be matched with experimental results in the early time of tracer injection. However, as time progresses, this difference becomes less. This trend may come from the assumption of negligible longitudinal dispersion in fracture and concentration difference between the fracture and fracture surface that was used in the analytical solution. Nevertheless, the numerical simulation model calibrated with experimental measurements of tracer concentration can be used to demonstrate the concentration difference between fracture and fracture surface. Figure 8a and b show that the numerical simulation results for the effluent concentration match very well with the experimental ones. This proves that the proposed modeling framework is working well. In addition, the numerical simulation model reveals the presence of solute

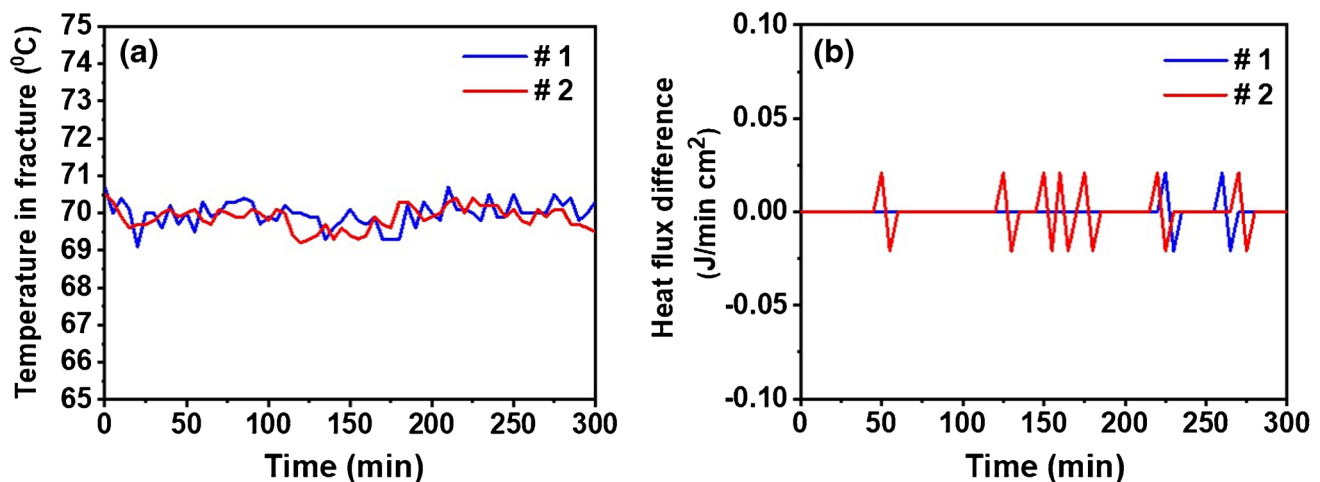


**Fig. 7** a Temperature in fracture and b heat flux changes measured in the middle of fracture for a flow rate of 1 ml/min at an initial temperature of 70 °C for different core plugs.



**Fig. 8** Comparison of tracer (Rhodamine-B) breakthrough curves for a flow rate of 1 ml/min at an initial temperature of 70 °C for core plugs **a** #1 and **b** #2

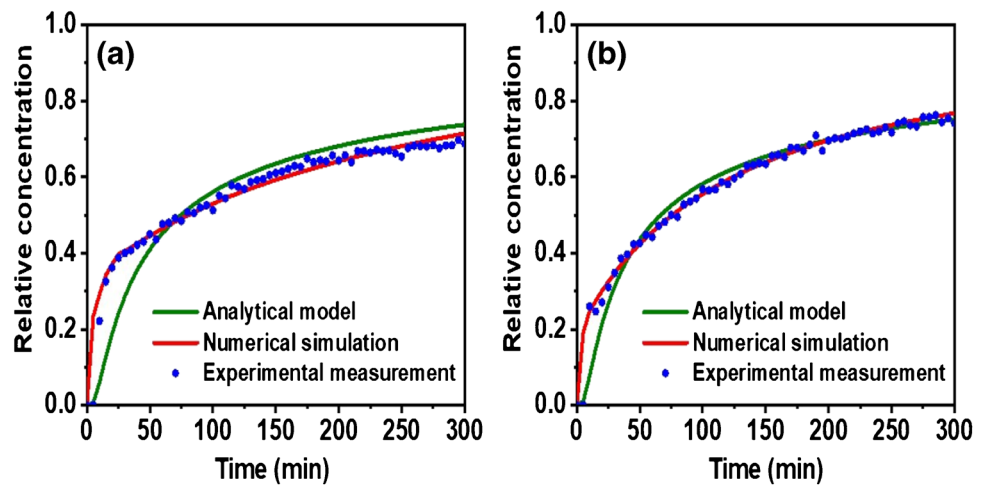
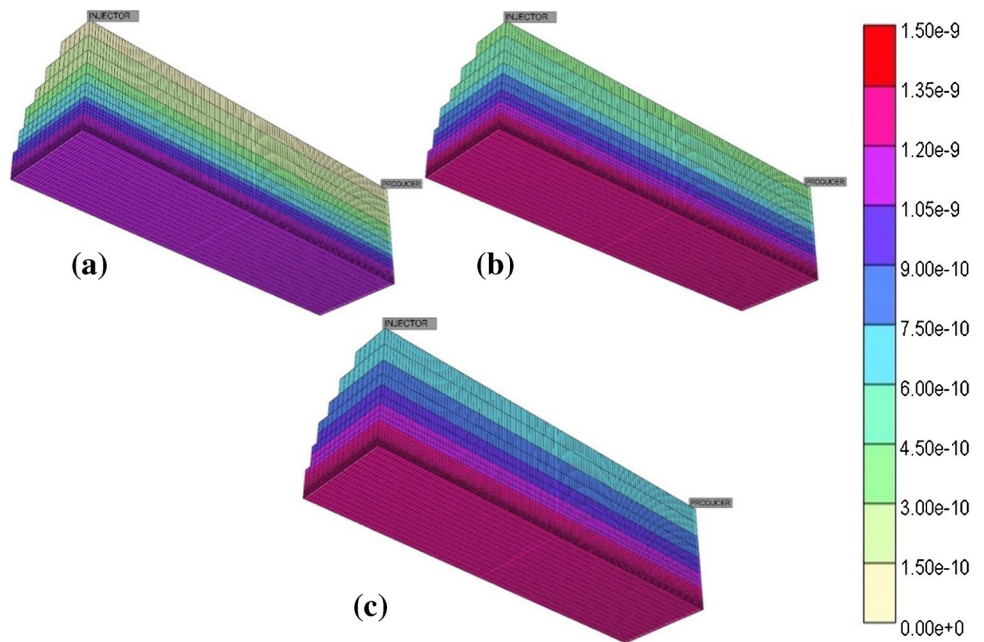


**Fig. 9** Distribution of tracer mole fraction in a single fracture matrix system for an injection rate of 2 ml/min at a temperature of 70 °C for core plug #1 at different injection times, **(a)** 60 min **(b)** 180 min **(c)** 300 min



concentration difference between the fracture and fracture surface as well as solute dispersion along the fracture. The numerical simulation model calibrated with experimental values was used to demonstrate how the tracer propagates into the matrix (Fig. 9). As can be seen, the tracer moves into the matrix uniformly. As time progresses, tracer concentration in the matrix increases.

The calibration of the numerical simulation model for matrix-fracture heat transfer with experimental values of temperature in fracture enables evaluation of the major contributing thermal properties of the matrix during the cold solute injection. Table 3 gives the values of matrix volumetric heat capacity and thermal conductivity for two different core plugs with different initial temperatures (i.e., 70 and 90 °C) (Tavakkoli Osgouei and Akin 2021). Increasing matrix thermal properties with an increasing outer

**Table 3** The thermal parameters used in matrix-fracture heat transfer (Tavakkoli Osgouei and Akin, 2021)

Core plug	Outer temperature (°C)	Matrix thermal conductivity (J/min cm °C)	Matrix volumetric heat capacity (J/cm <sup>3</sup> °C)
#1	70	3.5	12
	90	4.5	14
#2	70	1.9	5
	90	2.5	5.8

temperature of fractured core plugs indicates that the thermal behavior of the matrix is different affecting the amount of matrix-fracture heat transfer in non-isothermal conditions.

It is evident that the thermal properties of the matrix affect the temperature of the fracture surface, which has

a significant role in establishing a temperature gradient at the fracture-matrix interface. In a previous study, the sensitivity analysis was carried out to investigate the effect of injection rate and temperature on matrix-fracture transfers in different core plugs through a numerical model. Thus, different values of injection rate and outer temperature were selected for the sensitivity analysis. (Tavakkoli Osgouei and Akin 2021). Figure 10 demonstrates the influence of matrix thermal properties on matrix-fracture heat transfer for different initial temperatures of 70 and 90 °C. It can be observed that core plug #1 with larger values of thermal properties provides a higher temperature at the

fracture-matrix interface and a higher temperature gradient between fracture fluid and fracture surface.

A comparative analysis of measured and simulated results gives information about the transport parameters in matrix-fracture systems. The main controlling parameter recognized for history matching of the solute transport model is the dispersion coefficient. The values of the dispersion coefficient used to calibrate the analytical and numerical simulation model are given in Table 4. As opposed to a constant value of effective diffusion coefficient to fit the analytical model, different values of dispersion coefficients were assigned in the calibration of the numerical model (Table 4). The calibration determines a valid set of model parameters that

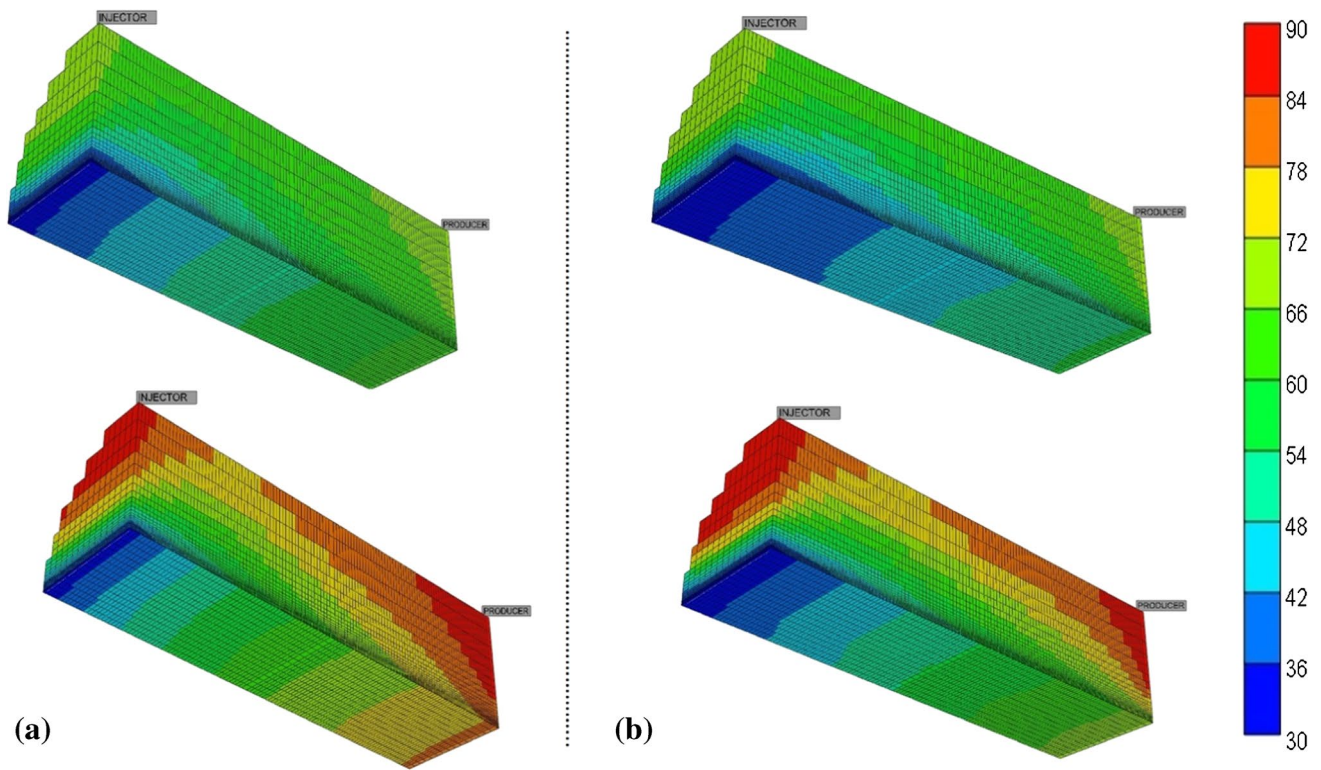


**Fig. 10** Temperature distribution in matrix-fracture system for a flow rate of rate 1.5 ml/min at different temperatures (70 °C and 90 °C) as a representative case of the sensitivity analysis for core plugs (a) #1 and (b) #2

**Table 4** The transport parameters used for calibration of the models

		Analytical Model	Numerical simulation model
Core plug	Matrix permeability (md)	Effective diffusion coefficient (cm <sup>2</sup> /min) ( $D_e$ )	Anisotropic dispersion coefficients (cm <sup>2</sup> /min) ( $D_x, D_y, D_z$ )
			$D_x$ 40 < $D_x$ < 70
			$D_y$ 50 < $D_y$ < 80
			$D_z$ 0.009 < $D_z$ < 1.3
# 1	8.39	0.73	0.0035 < $D_z$ < 0.75
# 2	3.79	0.59	

enables the use of a simulated model for the prediction of flow and/or transport behavior for different scenarios of matrix-fracture solute transport (Tunnish et al. 2019; Dietrich et al. 2005).

As can be observed from Table 4, the matrix permeability is the main factor controlling the amount of dispersion within the matrix. In fact, dispersion in the matrix enables tracer transfer from the fracture into the matrix over solute transport through fractured porous media. This can be clarified by the fact that the dispersion coefficient in the Z direction ( $D_z$ ) determines the amount of tracer penetration from fracture to matrix. Therefore, core plug #1 has more tracer compared to core plug #2. The level of solute penetration into the matrix for the two core plugs #1 and #2 with different values of matrix permeability and dispersion coefficient is shown in Fig. 11.

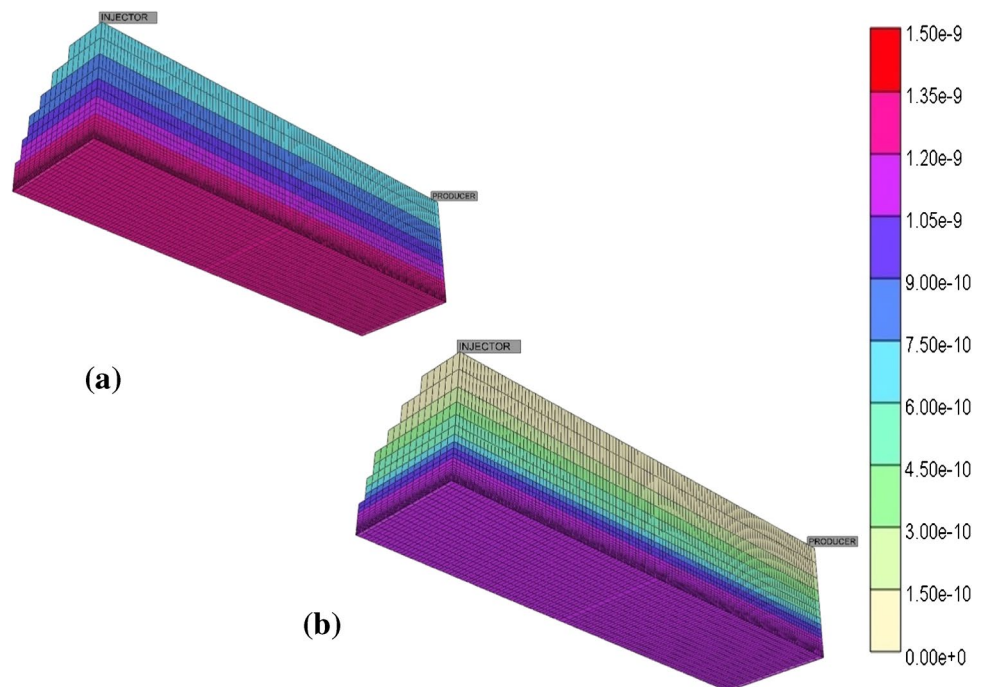
### Sensitivity analysis

The predicted tracer breakthrough concentration, steady concentration profile in fracture, steady concentration difference of fracture and fracture surface (matrix-fracture interface), and mass remaining in the matrix can be used as a diagnostic tool in the assessment of matrix-fracture transfers in non-isothermal conditions. Several runs were conducted to analyze the effect of changing the flow rate. The tracer breakthrough curves predicted for different injection rates of tracer at a constant outer temperature of 70 °C for core plug #2 illustrates that the effluent concentration increases with increasing injection rate (Fig. 12a). The tracer breakthrough

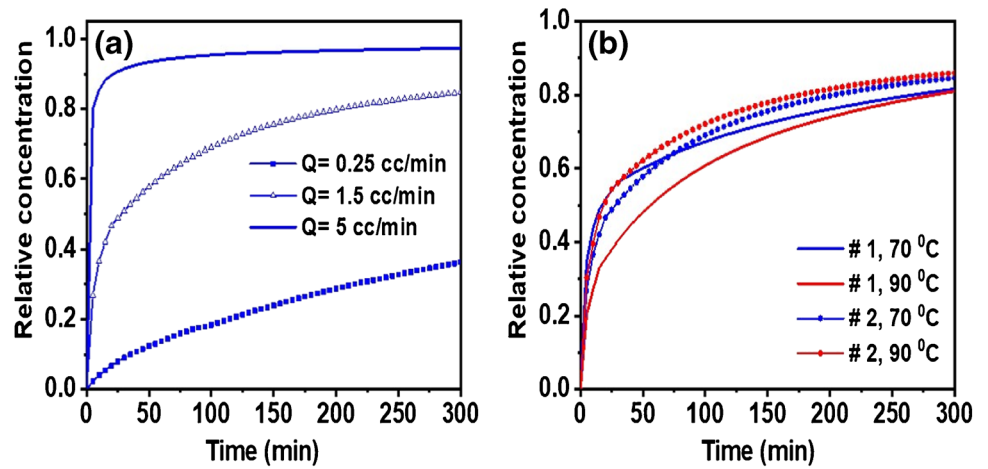
curve has a hyperbolic character that represents a relatively smaller solute penetration from the fracture into the porous matrix for a higher flow rate (i.e., 5 ml/min). In contrast, it changes to parabolic in nature due to greater solute penetration into the porous matrix at a smaller flow rate (i.e., 1.5 ml/min). At a very smaller flow rate (i.e., 0.25 ml/min), the tracer breakthrough curve is approximately linear resulting in the highest solute penetration into the matrix. A similar trend was observed for the predicted tracer breakthrough curves at different injection rates for core plug #1 simulations as well. The high injection rate decreases the contact time of the solute in fracture and fracture surface (matrix-fracture interface) that result in less solute penetration and an increase in relative outlet concentration. The resulting tracer concentration curve is steeper compared to that of the others. However, the tracer breakthrough curves become comparatively less steep with decreasing flow rate, reflecting an extended breakthrough curve as a result of high solute penetration into the porous matrix at a longer contact time.

Figure 12b shows predicted effluent breakthrough concentrations for a flow rate of 1.5 ml/min for different thermal properties of the matrix at two different initial temperatures. Because of the low dispersion coefficient, the core plug #2 has a higher relative effluent concentration compared to that of core plug #1 with high values of matrix permeability and dispersion coefficient. Although the physical properties of the matrix (i.e., matrix permeability) control solute transport in a single-fractured core plug, the tracer breakthrough curves change with changing initial temperature. Figure 12b illustrates that relative outlet concentration increases with

**Fig. 11** Distribution of tracer mole fraction in matrix-fracture system for an injection rate of 2 ml/min at a temperature of 70 °C at 300 min for core plugs, (a) #1 and (b) #2



**Fig. 12** **a** Simulated tracer breakthrough curves for different flow rates at an initial temperature of 70 °C for core plug #2. **b** Simulated tracer breakthrough curves for a flow rate of 1.5 ml/min at different initial temperatures (70 and 90 °C).



increasing initial temperature. The main reason for the effluent concentration changes can be attributed to the Soret effect. Mass flux from the fracture to the matrix due to a larger temperature gradient is larger in a matrix-fracture system for non-isothermal flow. Thermal properties of the matrix have a pivotal role on solute transport in matrix-fracture systems (Tavakkoli Osgouei and Akin, 2021). Figure 12b indicates that the changes in tracer breakthrough curves follow different trends at different temperatures. It is evident that there is an increasing trend in the breakthrough curve for core plug #2 as opposed to core plug #1 that has a decreasing trend with increasing initial temperature. The coupled heat and mass transfer with the Soret effect makes it possible to explain the different trends for different single-fractured core plugs with differing thermal properties. It can be observed that the thermal properties of the matrix are temperature-dependent variables, and the values of thermal properties of the matrix increase with increasing initial temperature from 70 to 90 °C (Fig. 10). Table 5 shows the amount of increase of thermal properties when the initial temperature increases from 70 to 90 °C. The increase in the values of thermal properties in core plug #1 is higher than that of core plug #2. Thus, high temperature over the fracture surface (matrix-fracture interface) contributes to a high-temperature gradient between fracture fluid and fracture surface which in turn more solute migrates toward the fracture surface (matrix-fracture interface) due to the Soret effect. As a result, the final effluent concentration decreases in core plug #1. In contrast, in core plug #2, heat storage in

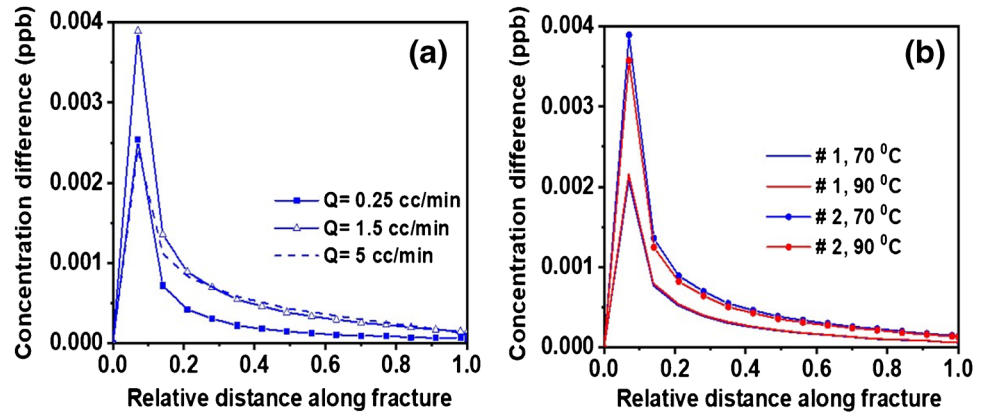
the matrix and temperature of the fracture surface becomes low (Table 5). Therefore, the Soret effect is less due to a low-temperature gradient between fracture fluid and fracture surface. Accordingly, the final effluent concentration is larger in the case of core plug #2 for an initial temperature of 90 °C (Fig. 12b).

The steady concentration difference between a fracture and fracture surface for different tracer injection rates at an initial temperature of 70 °C for core plug #2 is shown in Fig. 13a. The concentration difference along matrix-fracture for different flow rates represents that the concentration difference at the inlet is higher than the rest of fracture. In fact, it decreases exponentially, approaching about zero at the outlet for both of the fractured core plugs. The main factor controlling the amount of concentration difference is the level of tracer penetration from the fracture into the matrix. The large concentration difference near the fracture inlet is likely due to larger solute diffusion into the porous matrix in this section compared to the rest of the fracture. Since fracture matrix heat transfer is higher due to the large temperature difference at the fracture inlet, more solute penetrates into the matrix (Tavakkoli Osgouei and Akin 2021). Actually, the diffusion decrease contributes to a decline in the difference in tracer concentration at the fracture matrix interface. As revealed by sensitivity analysis, the amount of concentration difference increases with rising injection rate, achieving the maximum value at flow rate 1.5 (ml/min) for the core plugs #1 and #2. This can be explained by the fact that the increase in flow rate causes a large concentration difference along

**Table 5** The rate of increase in the values of thermal properties of the matrix from outer temperature 70 to 90 °C (Tavakkoli Osgouei and Akin, 2021)

Core plug	Thermal properties of matrix	70 °C	90 °C	Increase rate
#1	Thermal conductivity (J/min cm °C)	3.5	4.5	1.0
	Volumetric heat capacity (J/cm <sup>3</sup> °C)	12	14	2.0
#2	Thermal conductivity (J/min cm °C)	1.9	2.5	0.6
	Volumetric heat capacity (J/cm <sup>3</sup> °C)	5	5.8	0.8

**Fig. 13** **a** Simulated steady tracer concentration differences at the matrix-fracture interface for different flow rates at an initial temperature of 70 °C for core plug #2. **b** Simulated steady tracer concentration difference at the matrix-fracture interface for a flow rate of 1.5 ml/min at different initial temperatures (70 and 90 °C).

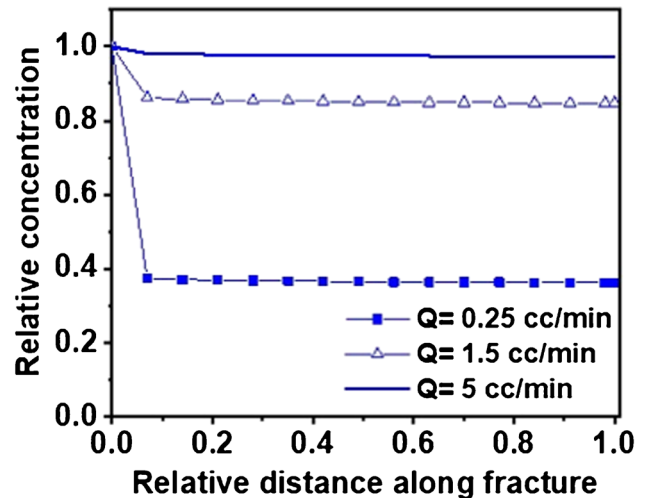


the fracture matrix interface due to larger diffusion into the porous matrix. As the flow rate is increased, the contact time decreases, and fracture surface (matrix-fracture interface) for higher flow rates leads to a decrease in solute diffusion into the matrix. Accordingly, this causes a decline in the trend of concentration difference (Fig. 13a).

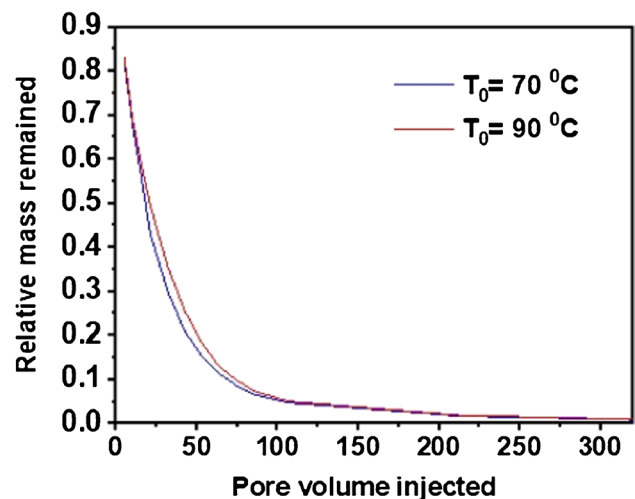
Because of the increase in outer temperature from 70 to 90 °C, the concentration difference in matrix-fracture interface follows different trends of changes in the two core plugs (Fig. 13b). This can come from the thermal properties of the matrix that is responsible for temperature gradient between fracture and fracture surface. In the case of core plug #2, the less Soret effect due to the low-temperature gradient between fracture fluid and fracture surface is the reason for the decrease in solute migration into the matrix and concentration difference at 90 °C. In contrast, the concentration difference increases slightly due to the larger Soret effect, causing a high amount of solute migration at 90 °C for core plug #1 over non-isothermal tracer injection processes.

Figure 14 represents the tracer concentration profile along a fracture in different flow rates at an outer temperature of 70 °C for core plug #2. The relative concentration undergoes a striking decline along a fracture in a low injection rate of 0.25 (ml/min) while it increases, approaching around 1.0 with a rising tracer injection rate to 5 (ml/min). Figure 14 indicates that the higher amount of decrease in relative concentration at lower flow rates can be caused by the longer contact time of solute in fracture with the matrix that is the reason for more solute penetration into the matrix. However, the relative concentration along fracture increases with a decrease in the level of solute penetration into the matrix in a shorter contact time because of the high injection rate of tracer through fracture-matrix systems.

To quantify the rate of solute transfer, the amount of solute remaining in the matrix is calculated. Knowing inlet and outlet concentrations ( $C_{in}$  and  $C_{out}$ ), time interval ( $\Delta t$ ), and the injection volume ( $V$ ), the mass flow rate ( $m^*$ ), and the mass ( $m$ ) of solute in the matrix can be calculated by using a mass balance (Bergman et al. 1992; Bird et al. 2002):



**Fig. 14** Simulated steady tracer concentration profiles along fracture for different flow rates at an initial temperature of 70 °C for core plug #2



**Fig. 15** Simulated mass remaining in the matrix as a function of pore volumes injected for different initial temperatures, core plug #1

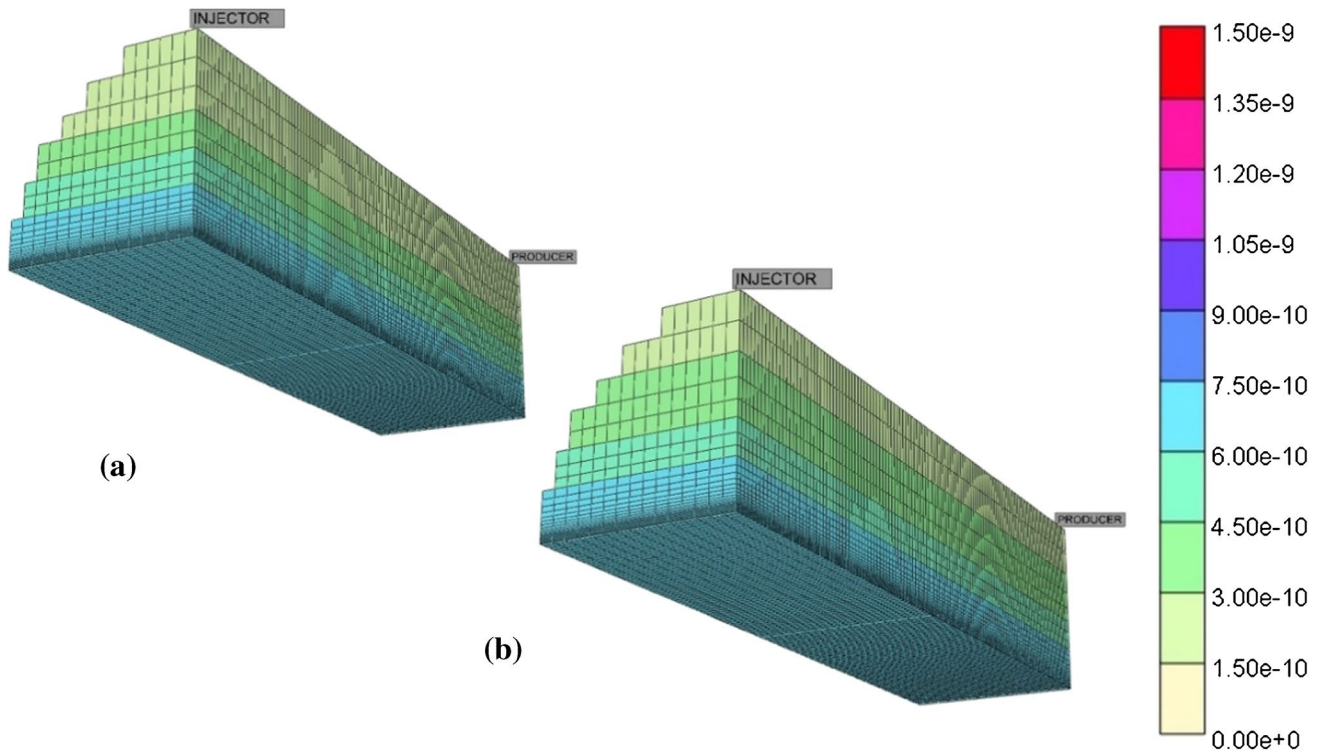


**Fig. 16** Distribution of tracer mole fraction in matrix-fracture system for an injection rate of 1.5 ml/min at 300 min for core plug #1 for different temperatures (a) 70 °C; (b) 90 °C

$$\frac{m^*}{V} = \frac{C_{in} - C_{out}}{\Delta t} \tag{9}$$

$$m = \sum (m^* \times \Delta t) \tag{10}$$

The mass remaining in the matrix can be affected by the thermal and physical properties of the matrix during solute transport in non-isothermal tracer injection processes. Mass balance was used to calculate the amount of solute remaining in the matrix at different pore volumes injected (flow rates) at inlet temperatures of 70 and 90 °C. The trend of mass remaining in the matrix for single-fractured core plug #1 is shown in Fig. 15. It can be seen that the amount of mass remaining in the matrix exponentially decreases with increasing pore volume injected (injection flow rate). In fact, shorter solute contact time at the fracture matrix interface in higher injection rates causes lower mass transfer, and the amount of mass in the matrix decreases. It can be also observed that the exponential decrease is somewhat different especially for low pore volumes injected for different initial temperatures. In view of the larger temperature gradient between fracture fluid and fracture surface in core plug #1, the Soret effect becomes more effective on matrix-fracture mass transfer. That is why the amount of mass remaining in the matrix increases as a result of more migration of solute

into the matrix at an outer temperature of 90 °C (Fig. 16). Thus, the Soret effect is more effective on the amount of mass remaining in the matrix at lower pore volumes injected (lower injection rates) for non-isothermal conditions.

The tracer breakthrough curves for different injection rates at different initial temperatures are shown in Fig. 17.

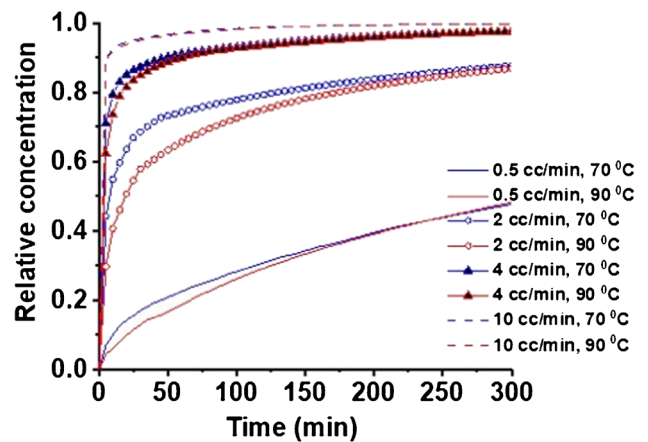


**Fig. 17** Simulated tracer breakthrough curves for different flow rates and outer temperatures, core plug # 1

These curves show that the difference between tracer breakthrough curves at higher flow rates is negligible compared to lower flow rates. Since the main reason for differences in outlet concentration of tracer at various outer temperatures is the Soret effect, it can be considered one of the most effective parameters in solute transport during non-isothermal tracer injection in a single-fractured porous media.

## Conclusions

Tracer flow experiments were conducted using two different synthetically created single-fractured limestone core plugs to investigate non-isothermal solute transport in a single fracture-matrix system. Conventional Rhodamine B tracer and suspension of micro particles based on melamine resin, Rhodamine B-marked size 1- $\mu\text{m}$  tracer was injected at a constant flow rate during non-isothermal flow-through experiments. Effluent tracer concentrations were measured using the fluorescence spectrometry technique. A numerical simulation model calibrated with experimental measurements was used to study coupled heat and mass transfers in a single-fractured matrix system at non-isothermal conditions. This calibrated simulation model was then used to determine effective thermal and physical properties involved in matrix-fracture transfers during tracer injection. The following conclusions were drawn.

- The tracer transfer from the fracture to the matrix at low injection rates is higher compared to that of higher injection rates.
- As the fracture provides a large transport pathway for micro particles compared to the surrounding matrix, advection as the predominant mechanism causes the early breakthrough for micro particle transport through a single fracture-matrix system.
- When the conventional tracer has a long enough transit through the system to diffuse into the matrix, but the micro tracer does not, the micro tracer arrives first and the conventional tracer later, and the separation measures the degree of preferential flow.
- Numerical studies indicated that matrix permeability is the main controlling factor for tracer dispersion within the matrix.
- Accurate modeling of non-isothermal tracer transfer from the fracture to the matrix requires consideration of the Soret effect.
- As opposed to the use of a constant dispersion coefficient, accurate description of fracture matrix mass transfer requires consideration of variable dispersion coefficients in different directions.

**Nomenclature**  $r$ : radius (cm);  $b$ : half aperture of fracture (cm);  $T_o$ : outer temperature of core plug ( $^{\circ}\text{C}$ );  $T_f$ : fluid temperature in fracture ( $^{\circ}\text{C}$ );  $T_i$ : initial temperature of core plug ( $^{\circ}\text{C}$ );  $T_{in}$ : inlet temperature of fluid ( $^{\circ}\text{C}$ );  $D_f$ : dispersion coefficient in fracture ( $\text{cm}^2/\text{min}$ );  $\alpha_L$ : longitudinal dispersivity in fracture (cm);  $u$ : fluid velocity (cm/min);  $D_m$ : molecular diffusion coefficient ( $\text{cm}^2/\text{min}$ );  $D_e$ : effective diffusion coefficient ( $\text{cm}^2/\text{min}$ );  $\tau$ : tortuosity of matrix;  $C_f$ : solute concentration in fracture (ppb);  $t$ : time (min);  $D_f$ : dispersion coefficient in fracture ( $\text{cm}^2/\text{min}$ );  $\emptyset$ : porosity (%);  $C_m$ : solute concentration in matrix (ppb);  $D_x$ : dispersion coefficient in x direction ( $\text{cm}^2/\text{min}$ );  $D_y$ : dispersion coefficient in y direction ( $\text{cm}^2/\text{min}$ );  $D_z$ : dispersion coefficient in z direction ( $\text{cm}^2/\text{min}$ );  $C_{in}$ : inlet concentration (ppb);  $C_{out}$ : outlet concentration (ppb);  $\Delta t$ : time interval (min);  $V$ : injection volume (lit);  $m^{\bullet}$ : mass flow rate ( $\mu\text{g}/\text{min}$ );  $m$ : mass of solute ( $\mu\text{g}$ ).

## Declarations

**Conflict of interest** The authors declare no competing interests.

## References

- Bergman TL, Incropera FP, DeWitt DP, Lavine AS (1992) Fundamentals of heat and mass transfer, 7th edn. John Wiley & Sons, New York, US
- Berre I, Doster F, Keilegavlen E (2019) Flow in fractured porous media: a review of conceptual models and discretization approaches. *Transport Porous Med* 130(1):215–236
- Bijeljic B, Rubin S, Scher H, Berkowitz B (2011) Non-Fickian transport porous media with bimodal structural heterogeneity. *J Contam Hydrol* 120:213–221
- Bird RB, Stewart WE, Lightfoot EN (2002) Transport phenomena, 2nd edn. John Wiley & Sons, New York, US
- Bodin J, Delay F, De Marsily G (2003) Solute transport in a single fracture with negligible matrix permeability: 1. fundamental mechanisms. *Hydrogeol. J.* 11(4), 418–433
- Boon M, Bijeljic B, Krevor S (2017) Observations of the impact of rock heterogeneity on solute spreading and mixing. *Water Resour Res* 53(6):4624–4642
- Boving TB, Grathwohl P (2001) Tracer diffusion coefficients in sedimentary rocks: correlation to porosity and hydraulic conductivity. *J Contam Hydrol* 53(1–2):85–100
- Charette VJ, Evangelista E, Chertcoff R, Auradou H, Hulin J-P, Ippolito I (2007) Influence of the disorder on solute dispersion in a flow channel. *Eur Phys J Appl Phys* 39(3):267–274
- CMG STARS Manual (2020) Advanced process and thermal reservoir simulator, CMG STARS, Computer Modelling Group Ltd., Calgary, AB, Calgary, Canada
- Dietrich P, Helmig R, Hötzl H, Sauter M, Köngeter J, Teutsch G (2005) Flow and transport in fractured porous media. Springer Science & Business Media, Berlin, Heidelberg
- Geiger S, Cortis A, Birkholzer J (2010) Upscaling solute transport in naturally fractured porous media with the continuous time random walk method. *Water Resour Res* 46(12):W12530
- Grisak G, Pickens J (1981) An analytical solution for solute transport through fractured media with matrix diffusion. *J Hydrol* 52(1–2):47–57
- Grisak G, Pickens J, Cherry J (1980) Solute transport through fractured media: 2. Column study of fractured till. *Water Resour. Res.* 16(4), 731–739
- Grisak GE, Pickens J-F (1980) Solute transport through fractured media: 1. The effect of matrix diffusion. *Water Resour. Res.* 16(4), 719–730

- Khuzhayorov B, Mustofokulov Z (2019) The adsorbed solute transport with diffusion effects. *J Appl Comput Math* 8(1):1–4
- Khuzhayorov B, Mustofokulov Z, Ibragimov G, Md Ali F, Fayziev B (2020) Solute transport in the element of fractured porous medium with an inhomogeneous porous block. *Symmetry* 12(6):1028
- Khuzhayorov B, Mustofokulov Z (2018) Transport of active solute in a fractured porous medium with nonequilibrium adsorption. *Int J Adv Res Sci Eng Technol* 5(12):7589–7597
- Kumar G (2012) A review on fluid dynamics of fractured reservoir geology. *Int J Geol* 6(2):45–52
- Olasolo P, Juárez M, Morales M, Liarte I (2016) Enhanced geothermal systems (EGS): a review. *Renew Sustain Energy Rev* 56:133–144
- Ramírez-Sabag J, Valdiviezo-Mijangos O, Coronado M (2005) Interwell tracer tests in oil reservoirs using different optimization methods: a field case. *Geofis Int* 44(1):113–120
- Reddy DS, Govardhan K (2015) Effect of viscous dissipation, solet and dufour effect on free convection heat and mass transfer from vertical surface in a porous medium. *Procedia Mater Sci* 10:563–571
- Reddy PS, Rao KS, Rao DP, Mamatha E (2010) Thermo-diffusion and diffusion–thermo effects on convective heat and mass transfer through a porous medium in a circular cylindrical annulus with quadratic density temperature variation—a finite element study. *Int J Dyn Fluid* 6(1):97–106
- Reddy PS, Rao V (2012) Thermo-diffusion and diffusion–thermo effects on convective heat and mass transfer through a porous medium in a circular cylindrical annulus with quadratic density temperature variation—finite element study. *J Appl Fluid Mech* 5(4):139–144
- Sahimi M (2011) *Flow and transport in porous media and fractured rock: from classical methods to modern approaches*, 2nd edn. John Wiley & Sons
- Schmelling S, Ross R (1989) Superfund ground-water issue. Contaminant transport in fractured media: Models for decision makers, Environmental Protection Agency, Washington, DC USA. Report EPA/540/4–89/004
- Tavakkoli Osgouei Y, Akin S (2021) Experimental and numerical study of flow and thermal transport in fractured rock. *Heat Mass Transf* 57:1053–1068. <https://doi.org/10.1007/s00231-020-03001-w>
- Tsang Y, Tsang C, Neretnieks I, Moreno L (1988) Flow and tracer transport in fractured media: a variable aperture channel model and its properties. *Water Resour Res* 24(12):2049–2060
- Tunnish A, Shirif E, Henni A (2019) History matching of experimental and CMG-STARs results. *J Petrol Explor Prod Technol* 9(1):341–351
- Werth CJ, Cirpka OA, Grathwohl P (2006) Enhanced mixing and reaction through flow focusing in heterogeneous porous media. *Water Resour Res* 42(12):W12414
- Zhu Y, Zhan H (2018) Quantification of solute penetration in an asymmetric fracture-matrix system. *J Hydrol* 563:586–598
- Zhu Y, Zhan H, Jin M (2016) Analytical solutions of solute transport in a fracture–matrix system with different reaction rates for fracture and matrix. *J Hydrol* 539:447–456
- Zou L, Jing L, Cvetkovic V (2016) Assumptions of the analytical solution for solute transport in a fracture-matrix system. *Int J Rock Mech Min Sci* 83:211–217

Springer Nature or its licensor (e.g. a society or other partner) holds exclusive rights to this article under a publishing agreement with the author(s) or other rightsholder(s); author self-archiving of the accepted manuscript version of this article is solely governed by the terms of such publishing agreement and applicable law.